FORMULATION OF NEAR AND FAR ACOUSTIC FIELD FROM AN INCOMPRESSIBLE FLOW FLUCTUATION AROUND THE RIGID WALL

Ki-Wahn Ryu* and **Duck-Joo Lee†**
Department of Aerospace Engineering,
Korea Advanced Institute of Science and Technology,
373-1, Kusong-Dong, Yusung-Ku, Taejon, 305-701, Korea

Abstract

A numerical study of a two-dimensional acoustic field is carried out for a spinning vortex pair located near a wall to investigate the effect of the wall from the spinning quadrupole source in unsteady vortical flows. Based on the unsteady hydrodynamic information from the known incompressible flow field, the perturbed compressible acoustic terms derived from the Euler equations are calculated. Non-reflecting boundary conditions on the free field and the solid boundary conditions are developed for a generalized curvilinear coordinates system to investigate the effect of a curved wall. It is concluded that the sound generated by the quadrupole sources of unsteady vortical flows in the presence of a flat wall or a circular cylinder can be calculated by using the source terms of hydrodynamic flow fluctuations in both near and far acoustic fields simultaneously.

1. Introduction

The motions of vorticity are considered to be directly related to the source of sound generated by vortical flows. These phenomena have been studied both theoretically[1-5] and numerically[6-7] by many researchers.

In accordance with the developments in computational fluid dynamics, computational aeroacoustics (CAA) provides a useful tool for analyzing the mechanism of aeroacoustic sound generation and propagation. There are several approaches in CAA to calculate the sound field. Direct simulation of Navier-Stokes equations is the most desirable method, but it requires a higher order numerical scheme. Some researchers solved the perturbed acoustic equations derived from the Euler equations to calculate propagation, scattering, or diffraction of incoming waves. However, the perturbed Euler equations cannot predict the sound generated by inherent unsteadiness of the flow because of the homogeneity of the equations.

Hardin and Pope[6] proposed a new computational aeroacoustics technique, where they split the Euler equations into hydrodynamic terms and perturbed acoustic terms. The novelty of their approach is found in the introduction of a new variable named 'hydrodynamic density fluctuations', which is the basic difference in the formulation of governing equations from others. They applied the technique to the problems of a pulsating and an oscillating sphere, which were acting as a monopole or a dipole source with sound-generating body surfaces.

In this paper, we are interested in the effect of a wall on the acoustic field generated by spinning vortices. A generalized curvilinear coordinates system is used to simulate the curved wall problem. This flow represents the basic model of the acoustic field generated by turbulent shear flows from the wall boundary layer. In the boundary layer, some coherent motions exist near the wall. These coherent motions affect the unsteady pressure fluctuations near the wall. The unsteady pressure fluctuations are strongly related to the near field sound, and parts of those energies are radiated to the far field acoustic energy. We would like to simulate near and far acoustic fields simultaneously.

2. Flow Field and Numerical Methods

The flow fields are simplified as an unsteady two-dimensional spinning vortex pair near the flat wall. The flow field can be assumed as a potential flow. The effect of the wall is represented by the mirror image method. Fig. 1 represents the schematic view of the spinning vortex pair on the flat wall with its image. The two point vortices, separated by a distance of $2r_0$ with circulation Γ, has a period $T = 8\pi^2 r_o^2/\Gamma$, rotation speed $\omega = \Gamma/(4\pi r_0^2)$, wave length $\lambda = \pi a_0/\omega$, and rotating Mach number $M_r = \Gamma/(4\pi r_0 a_0)$. A circular cylinder wall is also considered to investigate the curved wall effects.

Fig. 2 represents the schematic view of the spinning vortex pair around a circular cylinder with its image. It is well-known that the image method of the circular cylinder can be represented by the cir-

*Graduate Student
†Associate Professor

cle theorem. In this study, the center of the vortex pair is assumed to be fixed and the vortex pair rotates in a circular motion with radius r_0 in the flow field.

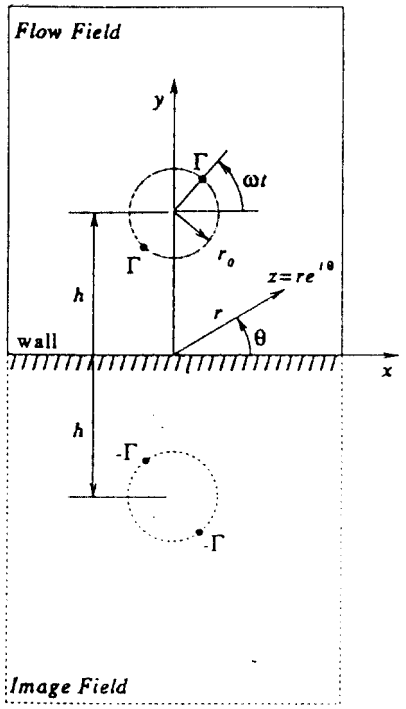

Fig. 1 Spinning vortex pair on a flat wall and its image.

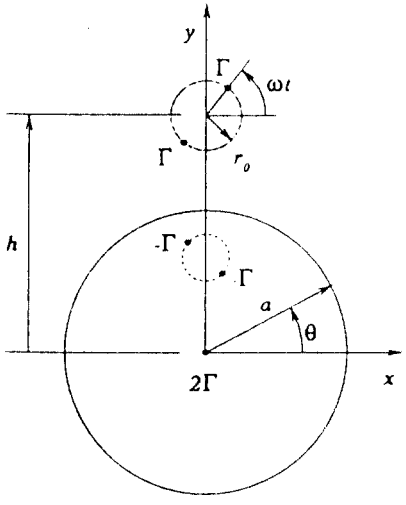

Fig. 2 Spinning vortex pair on a circular cylinder and its image.

In the numerical analysis for the acoustic field due to spinning vortices, a vortex core model is required to avoid the singularity at the center of the vortex. We use the Scully vortex model[8]. The Scully vortex model has smoother velocity distribution than the Rankine vortex model.

Boundary conditions are very important for acoustic problems. We used the non-reflecting boundary conditions based on the impedence condition on the free field boundary to account for the oblique wave on the free boundary. Thompson's technique[9] for a generalized coordinates system is used to obtain the density fluctuation. MacCormack's predictor-corrector scheme has gained wide use and acceptance for solving time-dependent problems in fluid dynamics and is used in the present study to integrate both the interior and the boundary points.

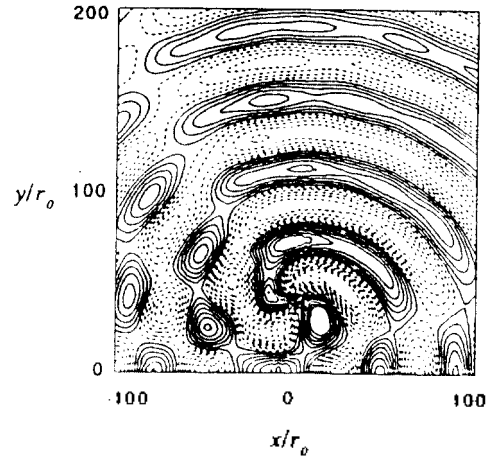

Fig. 3 Plot of the coustic pressure contour for $\Gamma/a_0 r_0 = 1$, $M_r = 0.0796$, $h/r_0 = 40$ at time $t = 10T$. The dashed line is negative value ($-2.5E-4 < p' < 2.5E-4$, 16-steps).

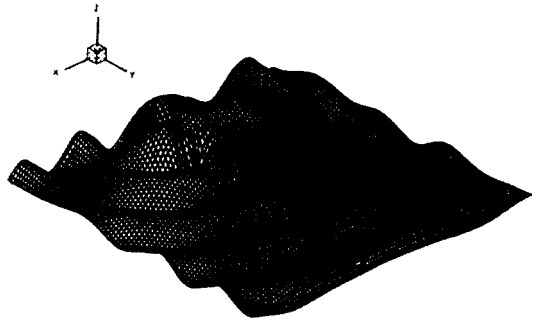

Fig. 4 Three-dimensional view of acoustic pressure for $\Gamma/a_0 r_0 = 1$, $M_r = 0.0796$, $h/r_0 = 40$ at time $t = 10T$. The upper-left side is wall boundary (z-direction represents the magnitude of $p' \times 200$).

3. Results and discussions

The computational domain has rectangular dimensions of $(L/r_0 \times L/r_0) = (200 \times 200)$ and grid system of 101×101. The spinning vortex is assumed to start abruptly at time $t = 0$. The rigid wall is located at $y/r_0 = 0$ as shown in Fig. 1, and the acoustic boundary conditions are, rigid wall boundary conditions.

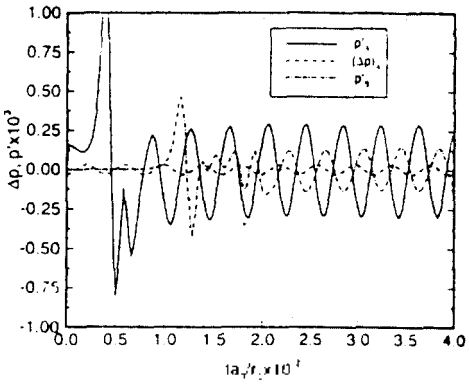

Fig. 5 Comparison of the acoustic pressure and wall pressure variation at the field point A, B according to time (point A: $(x/r_0, y/r_0) = (0,0)$, point B: $(x/r_0, y/r_0) = (100,100)$) for $\Gamma/a_0 r_0 = 1$, $M_r = 0.0796$, $h/r_0 = 40$ at time $t = 10T$.

Fig. 3 represents the acoustic pressure contours for a case of $\Gamma/a_0 r_0 = 1$, $M_r = 0.0796$, $h/r_0 = 40$. In this case, the distance from the wall to the acoustic source is nearly $1\lambda(\lambda/r_0 = 39.47)$. The three-dimensional graphical view is represented in Fig. 4. From the figures, we can observe the interaction phenomena between the waves from the spinning vortex pair and the reflecting waves from the rigid flat wall. Three series of the acoustic peaks on the left and one series of acoustic peak on the right are observed. In Fig. 3, the incident wave angles of the left field are greater than those of right field at that instant. For this reason, wave interference of the left field by the reflection wave becomes more severe than that of the right field. These phenomena break the symmetric directivity pattern of the spinning quadrupole source.

Fig. 5 represents the hydrodynamic pressure fluctuation and acoustic pressure variations on the wall (point A) and acoustic pressure variation in the field (point B) according to the non-dimensional time (point A: $(x/r_0, y/r_0) = (0,0)$, point B: $(x/r_0, y/r_0) = (100,100)$). The hydrodynamic pressure fluctuation is not larger than the acoustic pressure fluctuation at the wall (point A).

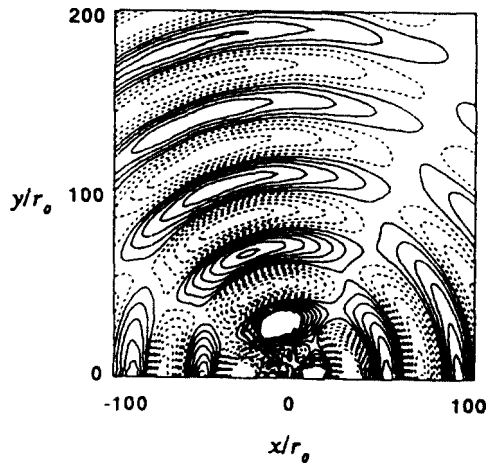

Fig. 6 Plot of the acoustic pressure contour for $\Gamma/a_0 r_0 = 1$, $M_r = 0.0796$, $h/r_0 = 4$ at time $t = 10T$. The dashed line is negative value $(-2.5E-4 < p' < 2.5E-4$, 16-steps).

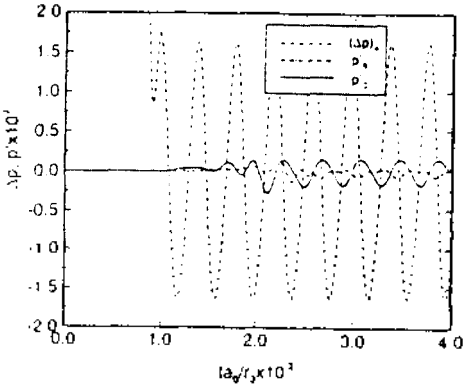

Fig. 7 Comparison of the acoustic pressures and wall pressure variation at the field point A, B and C according to time (point A: $(x/r_0, y/r_0) = (0,0)$, point B: $(x/r_0, y/r_0) = (100,100)$, and point C: $(x/r_0, y/r_0) = (0,104)$ which has $100r_0$ above the source) for $\Gamma/a_0 r_0 = 1$, $M_r = 0.0796$, $h/r_0 = 4$ at time $t = 10T$.

Fig. 6 represents the acoustic pressure contours for a case of $\Gamma/a_0 r_0 = 1$, $M_r = 0.0796$, $h/r_0 = 4$ which we can compare with the result of Fig. 3. The distance from the wall to the acoustic source is nearly 0.1λ. We can observe different series of acoustic peaks in left and right field. Fig. 7 represents the hydrodynamic pressure fluctuation and acoustic pressure variations on the wall (point A) and acoustic pressure variation in the field (point B) according to non-dimensional time (point A: $(x/r_0, y/r_0) = (0,0)$,

point B: $(x/r_0, y/r_0) = (100, 100)$, and point C: $(x/r_0, y/r_0) = (0, 104)$ which has $100r_0$ above the source). In this case, the hydrodynamic pressure fluctuation has a larger value than acoustic pressure fluctuation at the wall (point A). In spite of this main difference, the effect of acoustic source separation from the wall does not severely affect acoustic pressure fluctuation at the far field, as shown in Fig. 5 and Fig. 7.

Another numerical study is carried out for the circular cylinder wall to investigate the curvature effect of the rigid wall. The computational domain has an O-type body-fitted grid system (161 × 101). The distance from the origin of the circular cylinder to the far boundary is $9a$. We calculate the acoustic fields for the case of $\Gamma/a_0 r_0 = 0.02, M_r = 0.0796$ and $h/a = 2$ at $t = 15T$. Fig. 8 represents the acoustic density contours for the circular cylinder. From this figure, we can find the directivity pattern around the circular cylinder. As we realized from the flat wall, the scattered waves of the left field are more severe than those of right field.

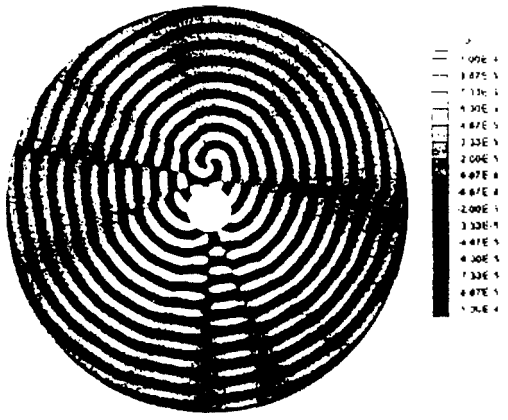

Fig. 8 Acoustic pressure contour around the cylinder for $\Gamma/a_0 a = 0.02$, $M_r = 0.0796$, and $h/a = 2$ at time $t = 15T$.

4. Conclusion

A computational aeroacoustic technique, which splits Euler equations into hydrodynamic terms and perturbed acoustic terms, is applied to the case of a spinning vortex pair near a flat or circular curved wall. It is found that the sound generated by the unsteady vortical flows in the presence of a body surface can be calculated by using the source terms due to the hydrodynamic pressure fluctuations. The spinning vortex pair in a free field generates a typical quadrupole directivity pattern, whereas for the spinning vortex pair near the wall, the acoustic directivity patterns show a scattering acoustic field due to the wall. From the above reason, a more silent zone can exist in the near field region as compared with the far field. It will be possible for the perturbed Euler equations based on the hydrodynamic density to be predicted more complex acoustic fields when the flow information is obtained.

References

[1]Powell, A., "Theory of Vortex Sound," *Journal of the Acoustical Society of America*, Vol. 36, No. 1, 1964, pp. 177-195.

[2]Müller, E. A., and Obermeier, F., "The Spinning Vortices as a Source of Sound," AGARD CP-22, 1967, pp. 22.1-22.8.

[3]Howe, M. S., "Contribution to the Theory of Aerodynamic Sound, with Application to excess Jet Noise and the Theory of the Flute," *Journal of Fluid Mechanics*, Vol. 71, 1975, pp. 625-673.

[4]Obermeier, F., "The Application of Singular Perturbations Methods to Aerodynamic Sound Generation," *Singular Perturbations and Boundary Layer Theory*, edited by Brouner, Gray and Mathieu, Springer-Verlag, Berlin, 1977, pp. 401-421.

[5]Yates, J. E., "Application of the Bernoulli Enthalpy Concept to the Study of Vortex Noise and Jet Impingement Noise," NASA CR2987, 1978.

[6]Hardin, J. C., and Pope, D. S., "A New Technique for Aerodynamic Noise Calculation," DGLR/AIAA 92-02-076, 1992.

[7]Lee, D. J. and Koo, S. O., "Numerical Study of Sound Generation Due to a Spinning Vortex Pair," *AIAA Journal* Vol. 33, No. 1, 1995, pp. 20-26.

[8]Scully, M. P., "Computational of helicopter Rotor Wake Geometry and Its Influence on Rotor Harmonic Airloads," MIT, Pub. ARSL TR 178-1, Cambridge, MA, March, 1975.

[9]Thompson, K. W., "Time Dependent Boundary Conditions for Hyperbolic Systems," *Journal of Computational Physics*, Vol. 68, 1987, pp. 1-24.